Received: 4 July 2023 | Revised: 14 November 2023 | Accepted: 24 November 2023

IET Power Electronics

DOI: 10.1049/pel2.12628

The Institution of Engineering and Technology WILEY

ORIGINAL RESEARCH

Experimental evaluation of the backstepping-based input resistance controller in step-up DC–DC converter for maximum power point tracking of the thermoelectric generators

Sarah Kowsari Mogadam[1] | **Mahdi Salimi**[2] | **Seyyed Mohammad Taghi Bathaee**[3] | **Davar Mirabasi**[1]

[1]Department of Electrical Engineering, Ardabil Branch, Islamic Azad University, Ardabil, Iran

[2]Faculty of Engineering and Science, University of Greenwich, Kent, UK

[3]Faculty of Electrical & Computer Engineering, K.N. Toosi University of Technology, Tehran, Iran

Correspondence
Mahdi Salimi, Faculty of Engineering and Science, University of Greenwich, Kent, ME4 4 TB, UK.
Email: m.salimi@gre.ac.uk

Abstract

In this paper, a novel non-linear model-based approach is presented for maximum power point (MPP) tracking of thermoelectric generators (TEGs) using the backstepping controller. Considering the output voltage range of the thermoelectric devices, a step-up DC–DC converter is employed as an interface between the load and input power source. According to the maximum power transfer theorem, if the equivalent input resistance of the converter (R_{in}) is equal to the internal resistance of the input source (R_{TEG}), the TEG operation at the MPP will be achieved. Hence, defining the R_{TEG} as a reference value and R_{in} as a feedback variable for a closed-loop controller, the backstepping non-linear controller is developed for input resistance control of the boost DC–DC converter. Owing to the non-linear nature of the error variable in the input resistance control of the converters, conventional linear controllers cannot guarantee the system's closed-loop stability within an extensive operational range. However, despite changes in generator's open-circuit voltage (V_{OC}) and R_{TEG}, the designed closed-loop controller can successfully stabilize the thermoelectric converter in different operational conditions. Considering the Lyapunov theorem and the Barbalat lemma, the asymptotic stability of the backstepping controller is proved. During the steady-state operation, the actual values of the V_{OC} and R_{TEG} are updated periodically by the measurement of the converter input voltage/current values. To verify the functionality of the designed control method, PC-based simulations are carried out in MATLAB/Simulink software. Moreover, by using TMS320F28335 digital signal processor from Texas Instruments and a simple thermoelectric simulator, the experimental response of the proposed controller is evaluated in dynamic and steady-state conditions. The developed closed-loop system can track the MPP of a TEG with zero steady-state error, regardless of uncertain parameter variations.

1 | INTRODUCTION

In recent years, the growing concern over global warming and its associated problems caused by the increasing reliance on fossil fuels has led to a heightened focus on the utilization of renewable and eco-friendly energy resources. A notable example is the widespread adoption of photovoltaic (PV) generators, which convert solar energy into electricity. Between 2016 and 2020, the global deployment of PV generators doubled, and it is projected that these generators will become the primary source of electricity by 2050 [1].

Similarly, the conversion of thermal energy directly into electrical power, known as the thermoelectric effect [2], has gained attention. One significant application of this concept is the recovery of dissipated heat in industrial processes using thermoelectric generators (TEGs) [3]. For instance, in hybrid electric

vehicles, incorporating a TEG system in the exhaust of an internal combustion engine can result in a 10% reduction in fuel consumption [4]. TEG systems have also been utilized in volcanic areas to generate electric power, leveraging the availability of hot mineral water [5].

Like PV systems, an important aspect of TEGs is the maximum power point tracking (MPPT) of the energy source. Since the output power profile of a TEG system is directly influenced by load and temperature, it is crucial to adjust the voltage and current of the generator under different conditions to achieve maximum power point (MPP) operation.

In the literature, numerous MPPT techniques for PV systems have been reported and compared [6]. One of the most commonly used methods is the Perturb and Observe (P&O) algorithm. In this technique, the operating point of the PV source is continuously perturbed during steady-state conditions. By comparing the PV output power before and after each perturbation, the next perturbation direction for MPPT can be determined. However, a major drawback of the P&O approach is the occurrence of steady-state oscillations in PV power [7].

To address this issue, model-based MPPT techniques have emerged in recent years [8]. These methods begin by defining an appropriate reference signal that ensures the MPP operation of the system. Considering the system model, a closed-loop controller is designed to regulate the output power of the PV modules. Given the voltage range of renewable energy generators, an interface step-up converter is employed between the input source and output load. Proper control of the input power to the converter is necessary for maximizing the output power.

While linear conventional controllers have been extensively used for MPPT of PV panels [9], their ability to regulate the closed-loop system effectively throughout an extensive operational range is limited due to the non-linear characteristics of power electronics converters. Consequently, employing a non-linear control method such as sliding mode [10] or a Lyapunov-based approach [11] proves advantageous.

To define a proper reference signal for the model-based MPPT controllers, at least four different approaches have been reported:

a. Application of the P&O algorithm for the calculation of the reference voltage/current of the step-up DC–DC converter [12]: Despite the simplicity, operating point and response of the system will be oscillatory in steady-state conditions.
b. Use of fractional open-circuit voltage or short-circuit current as a reference value [13]. This method may result in a large error value when the operating point of a closed-loop system is changed.
c. Employment of the converter input power derivative as a reference signal [14]. At MPP, the time derivative of converter input power must be zero under different operating conditions. Hence, it can be defined as a feedback signal in the closed-loop control system. In this approach, the controller reference is always zero. So, at MPP, an extra unit for the calculation of reference signal is no longer needed. However, the practical implementation of derivative block in a noisy environment of the power converters is not straightforward.
d. Calculation of reference current/voltage based on the ambient temperature and radiation level [6]. Due to the non-linear behaviour of PV panels and approximated nature of the models, the application of mentioned method may result in a significant error in different operational conditions.

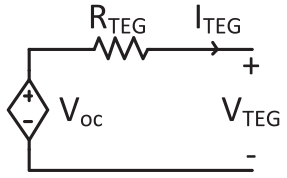

FIGURE 1 Electrical model of a TEG device. TEG, thermoelectric generator.

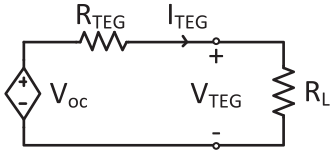

FIGURE 2 Power generation of the TEG device. TEG, thermoelectric generator.

Different from PV modules, the MPP voltage of a TEG device is exactly equal to half of the open-circuit voltage under different operating conditions. A similar approach is applicable for reference and the short-circuit currents of the TEG. Hence, if a model-based controller is employed for input voltage/current control of the step-up DC–DC converter, the reference value of the closed-loop system can be defined easily. For example, in [15], during the steady-state operation of the system, a time interval is introduced in the switching period for the measurement of the open-circuit voltage. In this interval, the output current of the TEG devices is zero which facilitates the measurement of the open-circuit voltage and updating of the reference value.

However, during the measurement interval in [15], the TEG is disconnected from the load and its output power is zero. To cope with this problem, it is possible to employ the buck or buck-boost DC–DC converters, which have pulsating input current waveform, for MPPT of the TEG devices [16]. In this condition, the power switch of the converter is in series with the TEG device. Therefore, while the main switch is OFF, the open-circuit voltage of the TEG can be monitored, and controller reference can be calculated without load interruption. It should be noted that utilization of the buck/boost as well as buck DC–DC converters for MPPT of the energy sources is not promising. Basically, in the mentioned converters, the input current is a pulsating waveform, and the operating point of TEG source will oscillate during the steady-state operation. Input current ripple can be decreased if a large electrolyte capacitor is employed as a filter in the input port of the converter. To monitor the open-circuit voltage, a switch in series

TABLE 1 TEG parameters in different temperatures.

	$\Delta T_1 = 5.5°C$	$\Delta T_2 = 10.7°C$	$\Delta T_3 = 15.3°C$	$\Delta T_4 = 20.1°C$	$\Delta T_5 = 25.6°C$
V_{oc}	18.3 V	35.8 V	51.1 V	67.3 V	84.9
R_{TEG}	132.6	132.7	133	133.2	133.5
$\alpha = (V_{oc})/(\Delta T)$	3.327	3.346	3.340	3.348	3.316

TEG, thermoelectric generator.

with the filter capacitor should be added which complicates the power topology as well as programming of the closed-loop system.

To modify the transient response of the controller in TEGs, a high-frequency injection plan is introduced in [17]. In this method, a high-frequency term is added to the duty cycle of the converter, which produces an offset in the TEG power. To settle at the MPP of the TEG, the value of the power offset is forced into zero by using a PI controller. The controller can be combined with the current MPPT approaches with any additional sensors. The gains of the PI controller are selected by trial and error. Hence, it is difficult to prove the plant stability while the converter operating point is changed widely. In [18], a linear extrapolation-based technique is developed for MPPT of the TEG devices under dynamically varying temperature conditions. In this method, random duty cycles are applied to the converter at first and changes in the MPP are computed based in the I–V characteristics of the TEG devices. Therefore, it is possible to supply the load during the calculation of open-circuit voltage continuously. In [18], for MPPT of the TEG devices, an open-loop controller is designed and the duty cycle at MPP is calculated based on the idealized steady-state behaviour of the converter. As a result, it is not valid during transient conditions. Also, parasitic elements of the step-up DC–DC converter, for example, series resistances of the inductor/switch/diode may play an important role at some operating points which are not considered in the open-loop idealized controller of [18]. To cope with this problem, the converter duty cycle should be determined at MPP through a closed-loop controller. In [19] and [20], different linear controllers are employed for the MPPT of the TEG devices. These approaches rely on the small-signal approximation around a fixed operating point. As a result, the mentioned linear controllers cannot guarantee the plant stability, if the converter operating point is changed widely.

Some novel methods have been developed for energy harvesting of the thermoelectric systems at MPP in recent years. In centralized TEGs, different local MPPs may be observed due to the non-uniform distribution of the temperature in TEG cells. To cope with this problem, a general regression neural network is employed in [21] for proper mapping between duty cycle as a control effort and input power of the chopper. The parameters of the neural network are tuned through the Bayesian optimization to improve the response of controller. However, long-term precise data is needed during the learning phase of the designed neural network. Also, hardware dependence is another drawback of the neural network in power electronics applications. In another word, considering the inherent mismatch of the TEG cells, each generator requires its own data and a general controller cannot be obtained by using artificial intelligence. A built-in input open-circuit voltage technique is developed for MPPT of the TEGs in [22]. To improve power efficiency of the generator, an adaptive term is added to the traditional single comparator-based controller of converter. The adaptive term of the duty cycle is calculated based on converter parameters and MPP voltage. As a result, exact values of the parameters for example, internal resistances of the inductor and switches are needed for the implementation of the designed approach. Also, a series switch on the input port of the converter is employed for the measurement of the open-circuit voltage. Hence, during measurement phase of the controller, input power of the converter is forced into zero. So, the converter will not be able to operate at MPP. It is well known that the slow dynamic response is the main drawback of the incremental resistance method. To cope with the mentioned problem in PV generators, the variable step size technique has been widely employed [23]. Recently, a similar approach in [24] has been adopted for TEGs according to the type-2 fuzzy logic-based method. Step response of the closed-loop system is evaluated while the load value and TEG temperature are changed. Compared to the conventional P&O approach, dynamic response of the designed controller is fast. Also, less oscillations are seen during the steady-state operation. However, according to the simulation results, the controller has considerable overshoot during step changes of the reference values. Also, in [25], a detailed design of a fuzzy logic controller is developed to modify the transient behaviour of the plant for MPPT as well as temperature control of a thermoelectric device. While it is employed as an electric power generator, the control is responsible for MPPT of the source. On the other hand, it can control the cold-side temperature when the thermoelectric device is functioning as a coolant equipment. However, the stability of the controllers in [24] and [25] is not studied in steady-state conditions. In another word, the accuracy of the fuzzy-based controllers can be compromised in power electronics applications due to wide changes of the system parameters.

The main contribution of this paper can be summarized as follows. In this article, a novel non-linear model-based controller is developed for MPPT of TEG devices using the backstepping controller. Considering the output voltage range of the thermoelectric devices, an interface step-up chopper is inserted between the load and input power source. Therefore, as input current waveform of the converter is smooth and non-pulsating, large and heavy filters are not needed at the input port of the converter. Considering the maximum power transfer theorem, if the equivalent input resistance of the converter (R_{in})

is equal to the internal resistance of the input source (R_{TEG}), the operation of the TEG at MPP could be achieved. Hence, by defining the R_{TEG} as a reference value and R_{in} as a feedback signal, the backstepping non-linear controller is developed for input resistance control of the step-up DC–DC chopper. Closed-loop control of the input resistance for MPPT of the TEG devices is a novel ideal, which has not been reported previously. It should be noted that due to non-linear nature of the error variable in input resistance control of the converters, conventional linear controllers cannot guarantee stability and robustness of the closed-loop system in a wide range of operations. Despite generator open-circuit voltage (V_{OC}) and R_{TEG} changes in an extensive range, the developed backstepping controller can stabilize the closed-loop plant satisfactorily. Considering the Lyapunov theorem, it is proved that the presented non-linear controller enjoys asymptotic stability in the whole operational conditions. During the steady-state operation, actual values of the V_{OC} and R_{TEG} are periodically updated by the measurement of the converter input power. To verify the functionality of the proposed control method, some PC-based simulations are carried out using the Matlab/Simulink. Moreover, by using TMS320F28335 DSP from Texas Instruments and a simple thermoelectric simulator, experimental behaviour of the developed backstepping controller is evaluated. The developed controller is able to maximize the TEG power with zero steady-state error, regardless of uncertain parameter variations.

The organization of the paper is as follows. First, the introduction of research and literature review is presented. In the next section, TEG modelling is briefly explained and verified through the small-scale experimental prototype. In Section 3, the state-space averaged model of the closed-loop system is extracted, and a novel non-linear resistance controller is developed for MPPT of the TEG source. The stability and robustness of the designed closed-loop system are proved using the Barbalat lemma. In this section, updating the model parameter and the calculation of TEG open-circuit voltage and internal resistance are explained. Finally, the simulation and experimental results of the developed closed-loop controller are presented.

2 | TEG MODELLING

2.1 | Electrical model

A TEG device includes the N- and P-type semiconductors in its structure, which convert input thermal energy directly into electrical power based Seebek effect. By series connection of TEG cells, a thermoelectric module is constructed, and its electrical model is shown in Figure 1 [26].

It should be noted that the open-circuit voltage value (V_{oc}) is related to the temperature gradient between the hot and cold sides (ΔT) of the TEG device as

$$V_{oc} = \text{ff}\Delta T \quad (1)$$

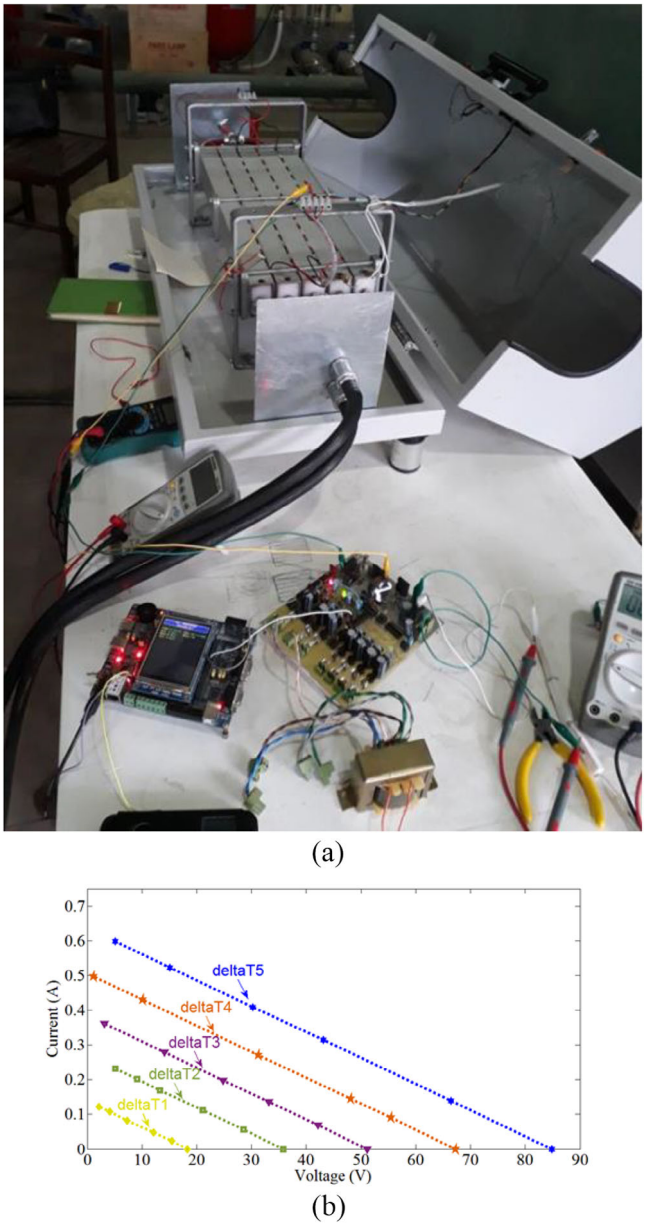

FIGURE 3 (a) The implemented TEG system. (b) Voltage–current characteristic of the implemented TEG in different temperatures. TEG, thermoelectric generator.

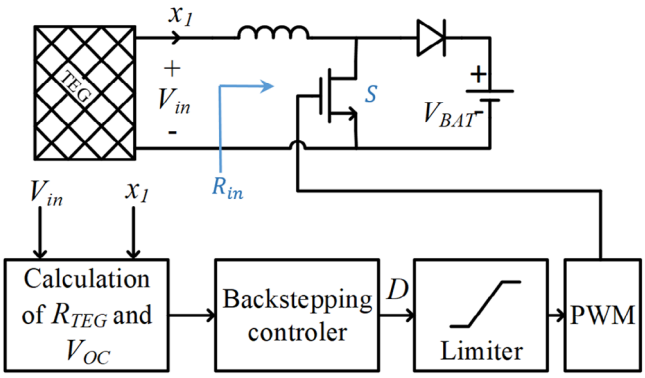

FIGURE 4 Structure of the proposed controller for input resistance control of the step-up chopper.

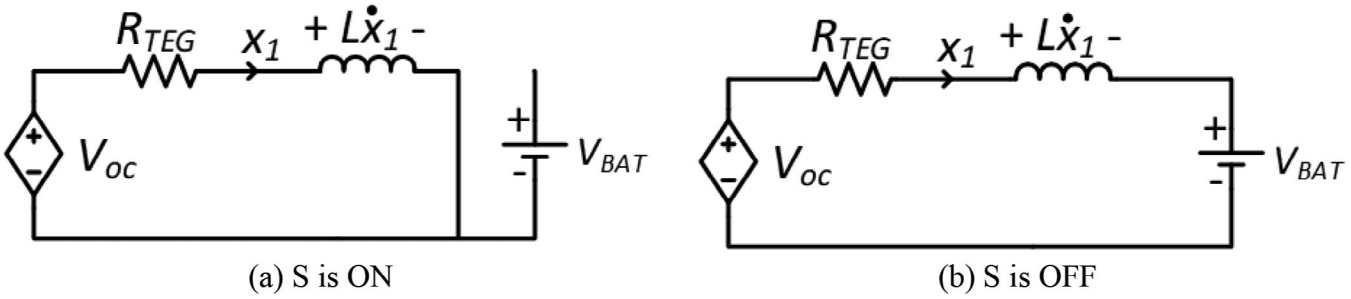

FIGURE 5 Equivalent circuit of the step-up chopper in different switching intervals. (a) S is ON, (b) S is OFF.

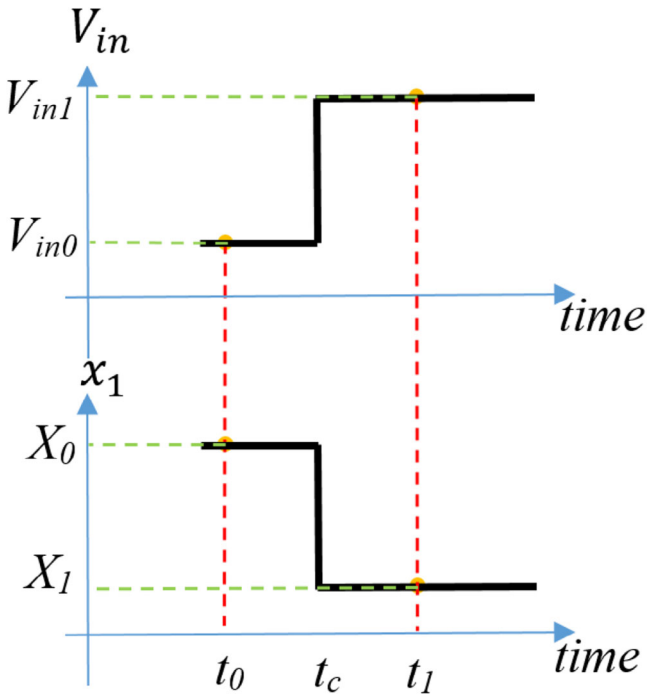

FIGURE 6 Updating the TEG parameters based on different operating points of the converter. TEG, thermoelectric generator.

where α is the Seebek coefficient and its value depends on the thermoelectric material type. Also, α may be slightly changed with ΔT [21]. Also, series resistance of the TEG device R_{TEG} changes with the temperature variations.

2.2 | MPP of the TEG

Considering Figure 2, TEG power can be calculated as follows where P_{TEG}, V_{TEG}, and I_{TEG} are the output power, terminal voltage, and output current of TEG, respectively. Also, R_L denotes the load resistance.

$$P_{TEG} = V_{TEG} \times I_{TEG} = \frac{R_L V_{OC}}{R_L + R_{TEG}} \times \frac{V_{OC}}{R_L + R_{TEG}} \quad (2)$$

It is clear that the TEG output power depends on the load value. Considering the maximum power transfer theorem, the load and the thermoelectric internal resistances must be equal at MPP:

$$\frac{dP_{TEG}}{dR_L} = 0 \Rightarrow \frac{(R_L - R_{TEG})}{(R_L + R_{TEG})^2} V_{oc}^2 = 0 \Rightarrow R_L = R_{TEG} \quad (3)$$

Clearly at MPP, $V_{TEG} = \frac{V_{OC}}{2}$ and $I_{TEG} = \frac{V_{OC}}{2R_{TEG}}$. So, if a controller is designed for input current regulation of the step-up chopper, the controller reference value must be selected as $x_1^* = I_{TEG}^* = \frac{V_{oc}}{2R_{TEG}}$ to ensure operation of the TEG at MPP. For input voltage controller, reference can be defined as $V_{TEG}^* = \frac{V_{OC}}{2}$. As in this paper, a closed-loop system is designed for input resistance control of the step-up DC–DC converter, reference value should be defined as $R_{in}^* = R_{TEG}$.

2.3 | Experimental analysis of the TEG parameters

In TEG devices, the values of the V_{OC} and R_{TEG} are changed with ΔT. To study this point experimentally, 48 thermoelectric modules (TEG12708) are connected in series. The photo of the laboratory setup, as well as voltage–current characteristic of the implemented TEG, which is measured in different temperatures are shown in Figure 3. According to Figure 1, the voltage–current characteristic of the thermoelectric modules can be written as follows:

$$V_{\mathrm{TEG}} = V_{\mathrm{oc}} - R_{\mathrm{TEG}} I_{\mathrm{TEG}} \quad (4)$$

Based on the experimental measurements, TEG model parameters in different temperatures are listed in Table 1.

Considering Equation (1) and behaviour of the TEG modules [27], it is seen that V_{oc} is directly increased with temperature. By fitting the polynomial functions based on the least-squares error, the open-circuit voltage can be expressed as follows in the operating range of the TEG:

$$V_{oc} = \left(-0.004428\Delta T^2 + 3.458\Delta T - 0.633\right) \approx (3.458\Delta T - 0.633) \quad (5)$$

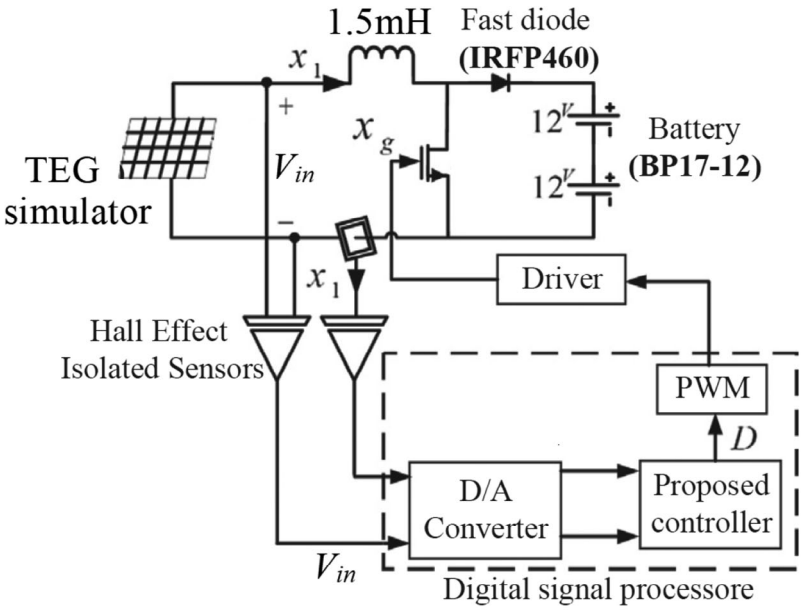

(a) Details of the practical setup

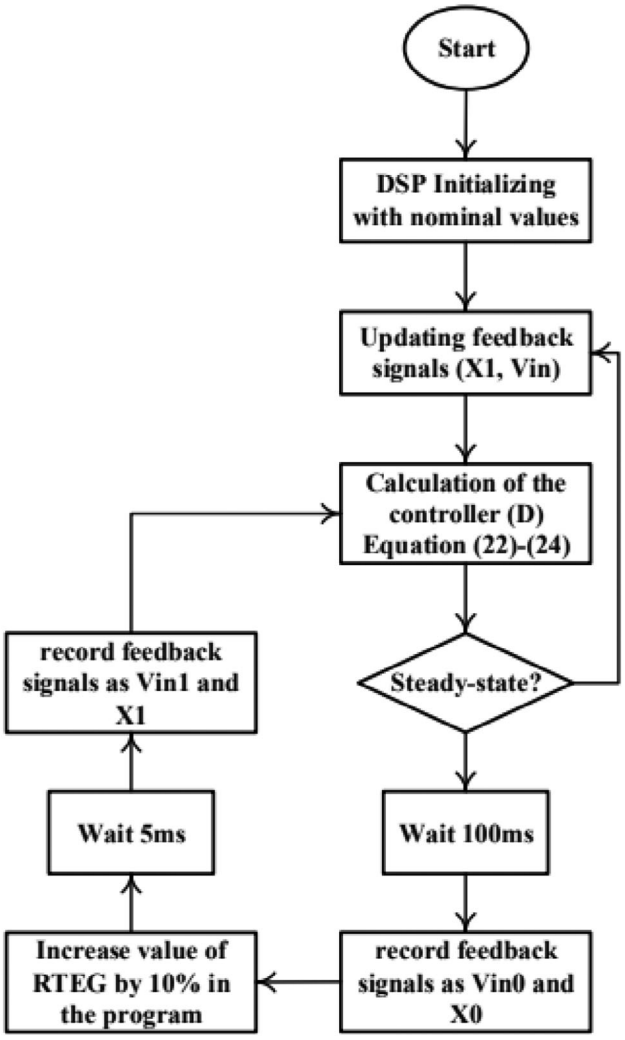

(b) Block diagram of the implemented controller

FIGURE 7 Experimental setup. (a) Details of the practical setup. (b) Block diagram of the implemented controller.

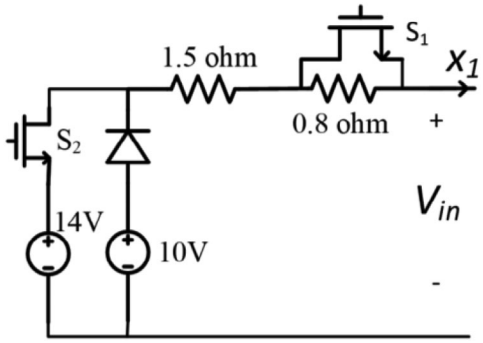

FIGURE 8 TEG simulator for the evaluation of the controller step response against R_{TEG} and V_{OC} changes. TEG, thermoelectric generator.

In addition, according to Table 1, the internal resistance R_{TEG} is almost fixed with respect to temperature changes. However, its variation can be modelled as

$$R_{TEG} = \left(0.0007404\Delta T^2 + 0.02329\Delta T + 132.4\right) \approx (0.04634\Delta T + 132.3) \quad (6)$$

Considering Equations (5) and (6), if a closed-loop system is designed for input current of the controller, the reference value at the MPP can be expressed as

$$x_1^* = \frac{V_{oc}}{2R_{TEG}} = \frac{3.32\Delta T + 0.2215}{0.04634\Delta T + 132.3} \quad (7)$$

According to (7), the calculation of the reference value based on the temperature measurement cannot precisely guarantee MPP operation of the TEG devices in a wide range of $\boldsymbol{\Delta T}$. Furthermore, it needs two monitoring sensors on both sides of the TEG device for temperature measurement. For this reason, the idea of input resistance control for MPPT of the TEG devices is considered in this article.

In Figure 4, the ideal of input resistance controller is illustrated using a step-up DC–DC converter. According to the maximum power transfer theorem, if input resistance of the chopper (R_{in}) and TEG internal resistance (R_{TEG}) have similar values, the MPP operation of the renewable generator will be guaranteed in different operating ranges. For this reason, the error variable of the controller is defined as follows:

$$e = R_{in}^* - R_{in} = R_{TEG} - R_{in} = R_{TEG} - \frac{V_{in}}{x_1} \quad (8)$$

where R_{in}^* is the reference value of the closed-loop system. Also, R_{in}, V_{in}, and x_1 denote the feedback signal, converter input voltage, and current respectively, and are defined in Figure 4. Considering inductor current (x_1) as a state variable, it is observed that the error variable has a non-linear relation with model state variables. For this reason, the application of the non-linear backstepping approach will result in a superior closed-loop behaviour, while equivalent input resistance of the converter is employed as the feedback signal. This method is developed by using the exact non-linear model of the system and does not need small-signal linearization. Feedback signals of the controller (R_{in}) are calculated based on the input current (x_1) and voltage (V_{in}) of the converter. Moreover, changes in the reference value (R_{in}^*) due to variations in the temperature are updated during steady state operation of the converter based on the feedback signals (x_1 and V_{in}) which are explained in the next section. The proposed non-linear controller determines duty cycle of the DC–DC converter so that the error variable is zero in different conditions, which guarantees the MPP operation of the TEG source. Value of the duty cycle is limited in the $0 \le D \le 1$ range and it is transformed into the switching signal (xg) through the PWM generator.

According to Figure 4, the system load (battery) which should be charged through the TEG source at MPP. The main objective of the controller design is input power regulation of the step-up chopper and MPPT of the TEG source. For this reason, load characteristic is not directly related to MPPT controller design [8].

3 | CLOSED-LOOP SYSTEM DESIGN

3.1 | System modelling

While the converter switch S is ON in Figure 4, the state-space model of the system can be written as follows based on the equivalent circuit of the chopper which is illustrated in Figure 5a.

$$\dot{x_1} = -\frac{R_{TEG}}{L}x_1 + \frac{V_{oc}}{L} \quad (9)$$

where x_1 is the inductor current. If the power switch is turned OFF, the initial inductor current will turn the diode ON. In this case, the equivalent circuit of the converter is shown in Figure 5b, and the system behaviour is given in Equation (9).

$$\dot{x_1} = -\frac{R_{TEG}}{L}x_1 + \frac{V_{oc}}{L} - \frac{V_{Bat}}{L} \quad (10)$$

where V_{Bat} denotes the load (battery) voltage. By multiplying Equation (9) in D and Equation (10) in $(1\text{-}D)$, the averaged state space model of the step-up chopper will be equal to [22]

$$\dot{x_1} = -\frac{R_{TEG}}{L}x_1 + \frac{V_{oc}}{L} - (1-D)\frac{V_{Bat}}{L} \quad (11)$$

3.2 | Backstepping controller design

The state-space model of the system has been extracted in the previous section in Equation (10). In this section, the input resistance control of the step-up DC–DC converter is

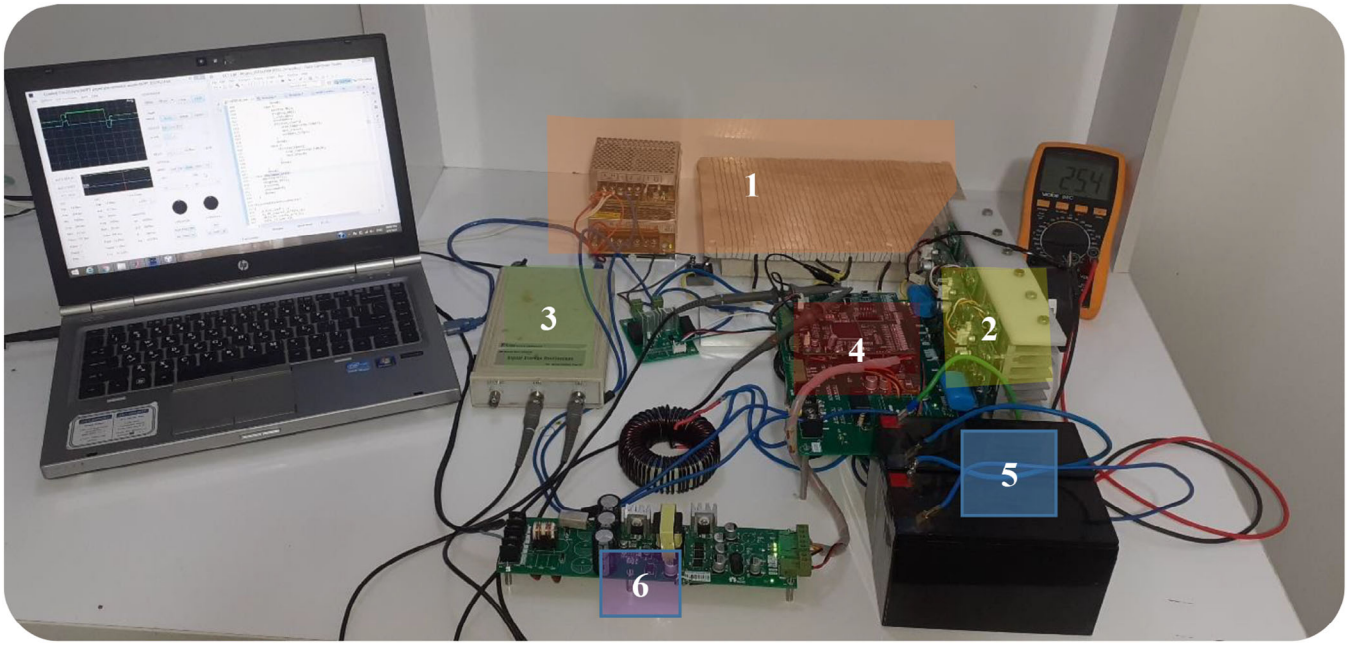

FIGURE 9 Test rig, 1—TEG simulator, 2—Step-up DC–DC converter, 3—20 MHz analogue PC-based oscilloscope (RS Pro 2205), 4—DSP board, 5—battery, 6—power supply. TEG, thermoelectric generator.

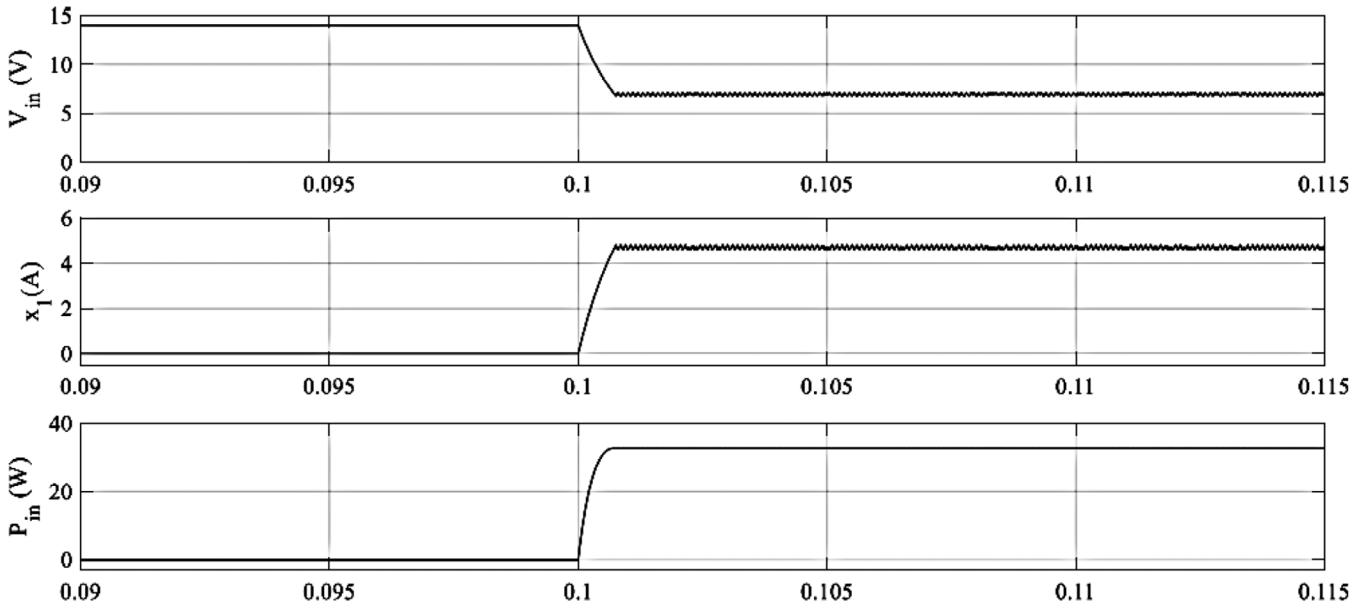

FIGURE 10 Simulation response of the controller during start-up.

presented using the non-linear backstepping controller for MPPT of the TEG sources. This controller is designed based on the Lyapunov stability theory and does not employ approximated small-signal models. For this reason, and due to the non-linear nature of the converter, the controller can stabilize the operating point of the converter robustly in a wide range of changes.

The input resistance error is defined in (8). By replacing V_{in} from Equation (4) in (8):

$$e = R_{TEG} - \frac{V_{oc} - R_{TEG}x_1}{x_1} = -\frac{V_{oc}}{x_1} + 2R_{TEG} \quad (12)$$

Considering the inductor current (x_1), as a state variable of the system, it is observed that the error variable has a non-linear nature. Hence compared with the inductor current controller design, input resistance regulation of the step-up chopper is more complicated. Although a linear controller can be developed by using a small-signal approximation, controller design

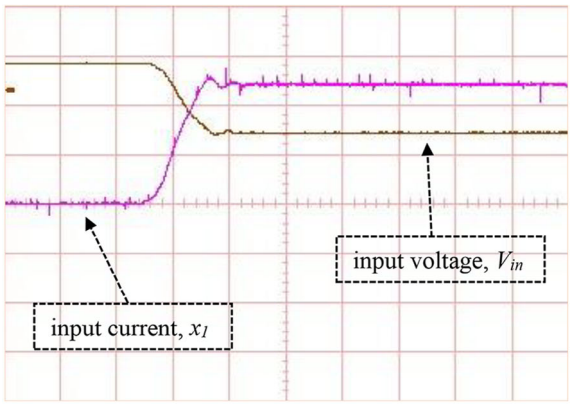

(a)

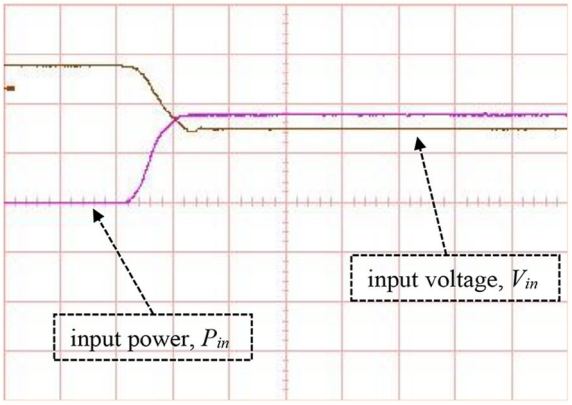

(b)

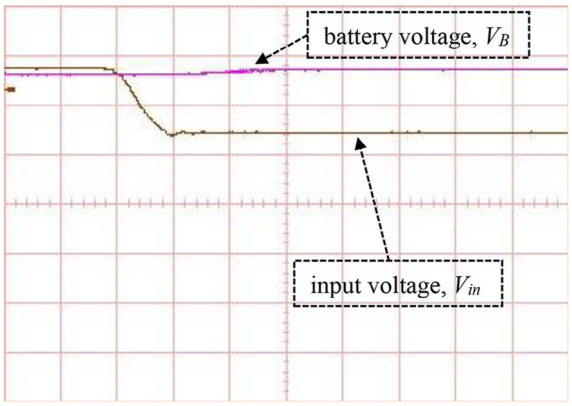

(c)

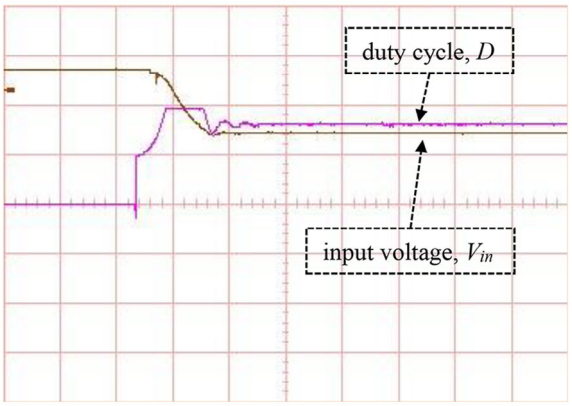

(d)

will only be valid around the operating point which cannot guarantee robustness of the closed-loop plant in different operating points.

To design the backstepping controller, $\dot{e}$ can be simplified as

$$\dot{e} = \frac{V_{oc}}{x_1^2}\dot{x}_1 \tag{13}$$

Replacing for $\dot{x}_1$ from (11), Equation (13) can be written as follows:

$$\dot{e} = \frac{V_{oc}}{x_1^2}\left(-\frac{R_{TEG}}{L}x_1 + \frac{V_{oc}}{L} - \frac{(1-D)\,V_B}{L}\right) \tag{14}$$

In this case, the Lyapunov function of the system can be chosen as follows:

$$V = \frac{1}{2}e^2 \tag{15}$$

As a result, the time derivative of the Lyapunov function will be equal to

$$\dot{V} = e\dot{e} \tag{16}$$

To guarantee the stability of the controller, $\dot{V}$ should be a semi-definite negative function. If it is assumed that $\dot{e} = -Ke$, then $\dot{V} = -Ke^2$ can be obtained. Assuming that the control parameter K is a positive scalar, then $\dot{V}$ will be a semi-definite negative function, and the stability of the system is secured. So, the controller should be designed to meet the following equation:

$$\dot{e} = -Ke \tag{17}$$

or:

$$\frac{V_{oc}}{x_1^2}\left(-\frac{R_{TEG}}{L}x_1 + \frac{V_{oc}}{L} - \frac{(1-D)\,V_B}{L}\right) = -K\left(-\frac{V_{oc}}{x_1} + 2R_{TEG}\right) \tag{18}$$

FIGURE 11 Dynamic response of the proposed non-linear resistance controller during start-up (time div. is 2.5 ms). (a) The input current, x_1 (2 A/div.), and input voltage, V_{in} (5 V/div.) changes during startup. It is observed that x_1 is zero and V_{in} = 14 V before running the controller. Also, during the steady-state operation, the system is settled on x_1 = 4.67 A and $V_{in} = \frac{V_{OC}}{2}$ = 7 V which is the MPP of the input source. (b) The input power, P_{in} (20 W/div.), and input voltage V_{in} (5 V/div.) change during startup. It is observed that P_{in} is zero before running the controller. Also, during the steady-state operation, the system is settled on $P_m = x_1\ V_{in}$ = 32.67 W which is the MPP of input source. (c) The battery voltage, V_B (10 V/div.) and input voltage V_{in} (5 V/div.) change during startup. It is observed that V_B slightly increases once the controller started due to voltage drop across the internal resistance of the battery. (d) The duty cycle, D (0.5/div.), and input voltage, V_{in} (5 V/div.) changes during startup. It is observed that the maximum value of the duty cycle is limited to 0.95 during the transient condition. MPP, maximum power point; TEG, thermoelectric generator.

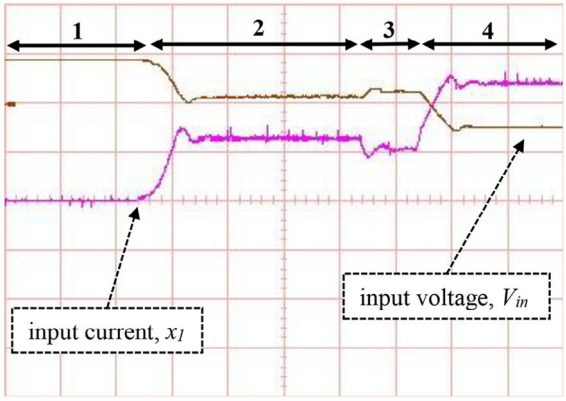

(a)

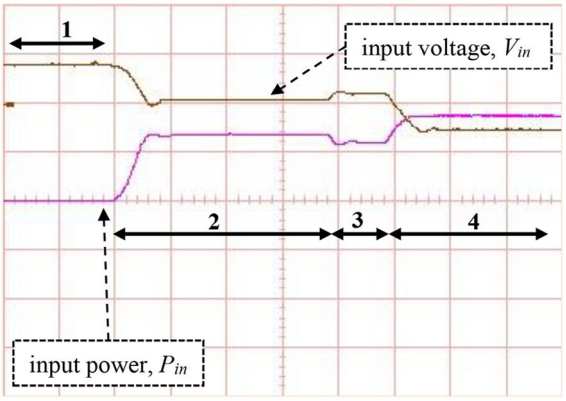

(b)

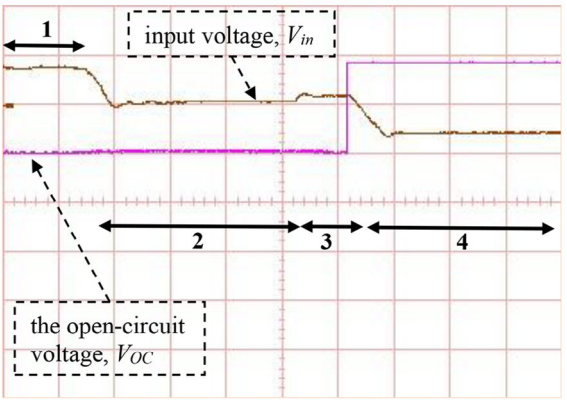

(c)

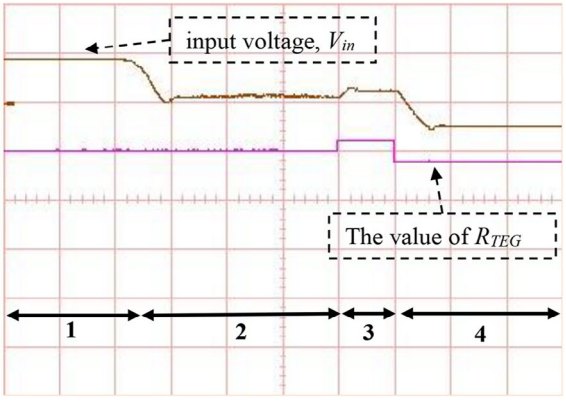

(d)

Considering (18), the controller can be simplified as follows:

$$D = 1 - \left(\frac{V_{oc}}{V_B} - \frac{R_{TEG} x_1}{V_B} - \frac{KL x_1}{V_B} + \frac{2KLR_{TEG} x_1^2}{V_B V_{oc}} \right) \quad (19)$$

In the steady-state condition, $x_1 = \frac{V_{oc}}{2R_{TEG}}$. By substituting this equation into (19), the steady-state behaviour of the proposed controller is obtained:

$$D_{ss} = 1 - \left(\frac{V_{oc}}{V_B} - \frac{R_{TEG} x_1}{V_B} \right) \quad (20)$$

or

$$D_{ss} = 1 - \frac{V_{oc} - R_{TEG} x_1}{V_B} = 1 - \frac{V_{in}}{V_B} \quad (21)$$

which is compatible with the steady-state characteristic of the step-up DC–DC converter. It should be noted that the D_{ss} is the duty cycle of the controller during steady-state operation.

So, the backstepping controller can be simplified as follows where the D_{dyn} is dynamic controlling component

$$D = D_{ss} + D_{dyn} \quad (22)$$

$$D_{ss} = 1 - \left(\frac{V_{oc}}{V_B} - \frac{R_{TEG} x_1}{V_B} \right) \quad (23)$$

$$D_{dyn} = \frac{KL x_1}{V_B} - \frac{2KLR_{TEG} x_1^2}{V_B V_{oc}} \quad (24)$$

Stability and robustness of the proposed backstepping controller can be investigated using the Barbalat lemma [28]. According to these criteria, if:

1. The Lyapunov function V is lower-bounded

FIGURE 12 Experimental dynamic response of the proposed non-linear resistance controller during start-up with unknown parameters of the TEG source (time div. is 2.5 ms). (a) The input current, x_1 (2A/div.), and input voltage, V_{in} (5 V/div.) changes during startup. The closed-loop system includes four different intervals as follows: Interval 1: Converter is OFF. It is observed that x_1 is zero and $V_{in} = 14$ V before running the controller. Interval 2: Converter starts with unknown parameters. Interval 3: TEG parameters are calculated. Interval 4: Converter tracks the MPP. The system is settled on $x_1 = 4.67$ A and $V_{in} = \frac{V_{OC}}{2} = 7$ V which is the MPP of the input source. (b) The input power, P_{in} (20 W/div.), and input voltage V_{in} (5 V/div.) change during startup. It is observed that P_{in} is zero within the first interval before running the controller. Finally, the system is settled on $P_m = x_1 V_{in} = 32.67$ W within interval 4 which is the MPP of input source. (c) The value of the open-circuit voltage, V_{OC} (5 V/div.) and input voltage, V_{in} (5 V/div.) are illustrated. It is observed that the initial value of $V_{OC} = 5$ V is assumed as an initial value of the open-circuit voltage and it is updated to $V_{OC} = 14$ V within the interval 3 which is the actual value of the parameter. (d) The value of R_{TEG} (2 Ω/div.) and input voltage, V_{in} (5 V/div.) are illustrated. It is observed that the initial value of $R_{TEG} = 2$ Ω is assumed as an initial value of the TEG internal resistance and it is updated to $R_{TEG} = 1.5$ Ω within the interval 3 which is the actual value of the parameter. MPP, maximum power point; TEG, thermoelectric generator.

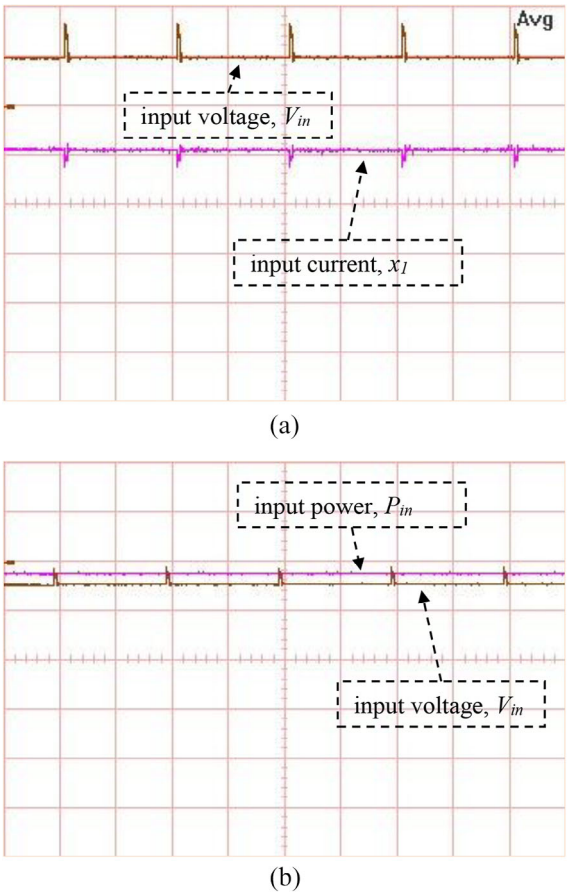

FIGURE 13 Experimental response of the controller during steady-state operation (time div. is 50 ms). The value of the R_{TEG} is changed (15%) each 100 ms in the DSP codes to determine the possible variations of TEG parameters (time div. is 50 ms). (a) The input current, x_1 (4 A/div.), and input voltage, V_{in} (2.5 V/div.) changes during steady-state operation due to changes in R_{TEG} value in the DSP codes. (b) The input power, P_{in} (20 W/div.) and input voltage V_{in} (5 V/div.) change during steady-state operation due to changes in R_{TEG} value in the DSP codes. DSP, digital signal processor; TEG, thermoelectric generator.

2. Time derivate of the Lyapunov function $\dot{V}$ is a uniformly continuous semi-definite negative function

Then in the steady-state operation of the converter, $\dot{V} = -Ke^2$ will be equal to zero.

To check the mentioned lemma, it is enough to investigate uniform continuity of $\dot{V}$. According to $\dot{V} = -Ke^2$, the time derivative of the $\dot{V}$ can be simplified as follows:

$$\ddot{V} = -2Ke\dot{e} \tag{25}$$

By replacing for e and $\dot{e}$ from (12) and (14) in (25)

$$\ddot{V} = -2K\left(-\frac{V_{oc}}{x_1} + 2R_{TEG}\right)\left[\frac{V_{oc}}{x_1^2}\left(-\frac{R_{TEG}}{L}x_1 + \frac{V_{oc}}{L} - \frac{(1-D)V_B}{L}\right)\right] \tag{26}$$

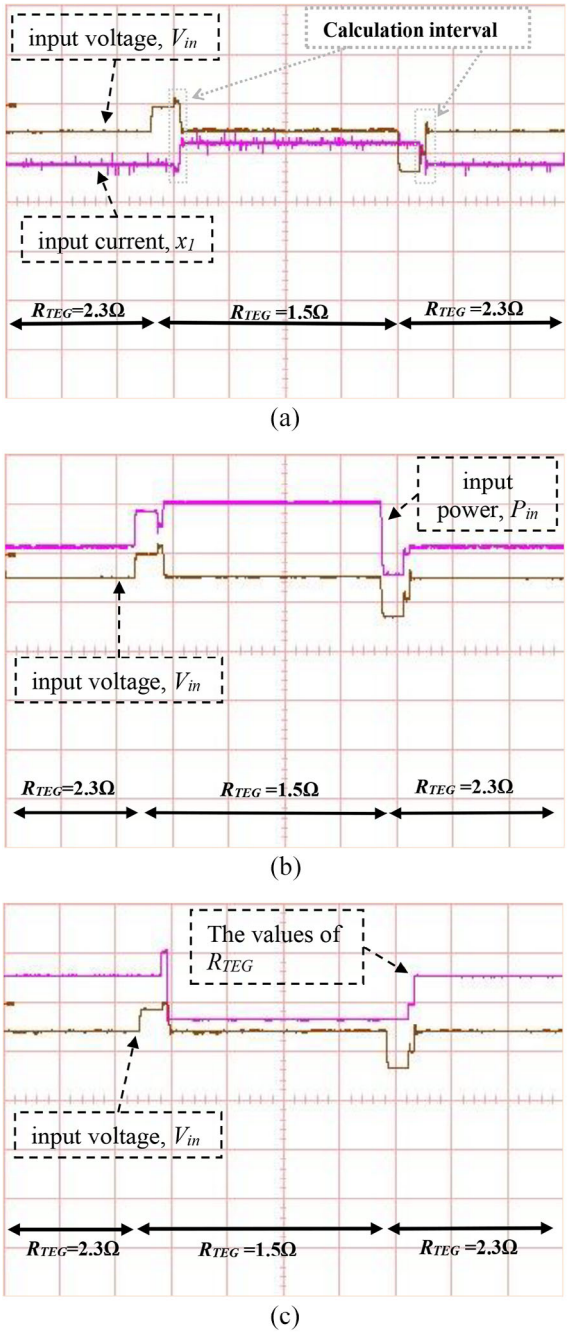

FIGURE 14 Experimental response of the controller during step changes of the TEG internal resistance (time div. is 25 ms). (a) The input current, x_1 (4 A/div.), and input voltage, V_{in} (5 V/div.) graphs during step changes of R_{TEG}. Apart from the calculation interval, it is observed that $V_{in} = 7\ V$ which proves MPP operation. (b) The input power, P_{in} (10 W/div.), and input voltage V_{in} (5 V/div.) graphs during step changes of R_{TEG}. It is seen that the measured input power is compatible with the maximum power point equation ($P_{in} = \frac{V_{in}^2}{R_{TEG}}$) for different R_{TEG} values. (c) The values of R_{TEG} (1 Ω/div.) and input voltage, V_{in} (5 V/div.) are illustrated. It is seen that the calculation is compatible with the real R_{TEG} values in different operating points. MPP, maximum power point; TEG, thermoelectric generator.

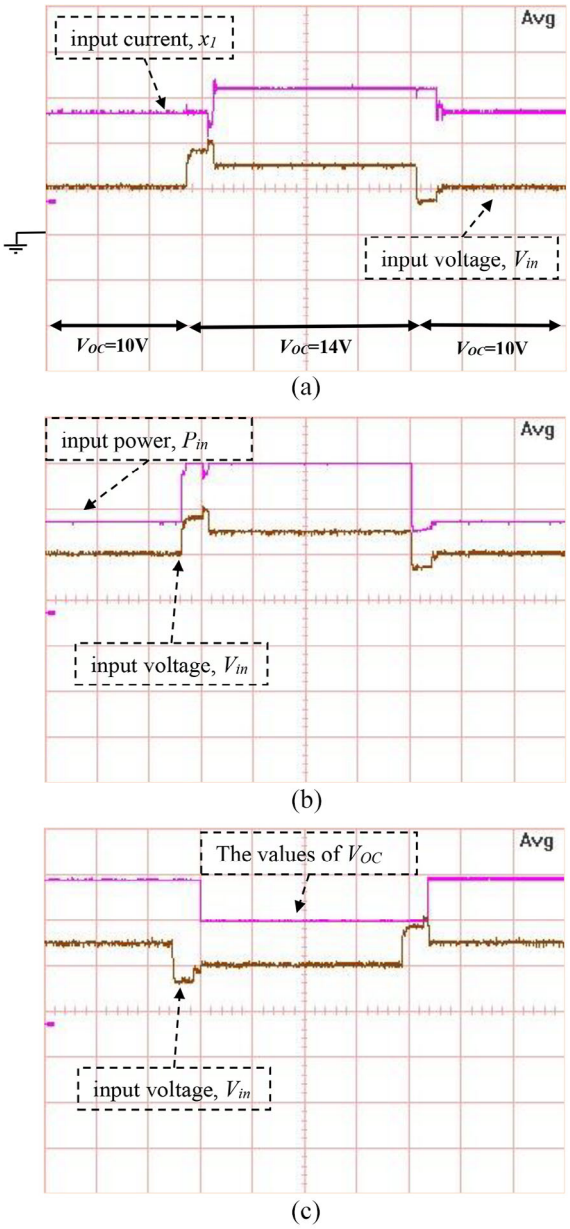

FIGURE 15 Experimental response of the controller against step changes of the TEG open-circuit voltage (time div. is 25 ms). (a) The input current, x_1 (2 A/div.) and input voltage, V_{in} (5 V/div.) graphs during the step changes of open-circuit voltage (V_{OC}). It is observed that the input voltage is equal to $V_{in} = \frac{V_{OC}}{2}$ in different operating points which proves the MPP operation of designed controller. (b) The input power, P_{in} (10 W/div.), and input voltage V_{in} (5 V/div.) graphs during step changes of open-circuit voltage (V_{OC}). It is seen that the measured input power is compatible with the maximum power point equation ($P_{in} = \frac{V_{OC}^2}{4R_{TEG}}$) for different V_{OC} values. (c) The values of V_{OC} (5 V/div.) and input voltage, V_{in} (5 V/div.) are illustrated. It is seen that the calculation is compatible with the real V_{OC} values in different operating points. MPP, maximum power point; TEG, thermoelectric generator.

As all the parameters in (25) including state variable, model parameters, controller gain, and control effort are all bounded, hence $\ddot{V}$ is a bounded function. So, the $\ddot{V}$ will be a uniformly continuous function. Considering the Barbalat lemma and regardless of the converter operating point

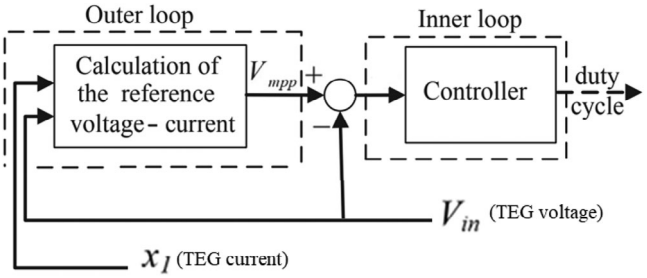

FIGURE 16 The P&O-based two-loop MPPT control approach. MPPT, maximum power point tracking; P&O, perturb and observe.

and changes in the parameters, the proposed closed-loop controller will be asymptotically stable with zero steady-state error.

3.3 | Updating the model parameters

As inductor current is equal to $x_1 = \frac{V_{oc}}{2R_{TEG}}$ at the MPP, so in the designed controller, the values of the V_{oc} and R_{TEG} determine the MPP of the TEG system. Although the controller starts with the nominal values of the mentioned parameter (based on normal temperature gradient), it is required to calculate actual values of the V_{oc} and R_{TEG} during the steady-state operation of the system to ensure MPPT. To calculate actual values of the TEG parameters, the value of the R_{TEG} is increased by 10% in the DSP codes during steady-state operation of the controller and then, V_{in} and x_1 are measured through the sensors, before and after changes in the R_{TEG}.

According to Figure 6, the value of the R_{TEG} is increased in the DSP codes on $t = t_c$ by 10%. In this Figure 6, X_0 and X_1 are values of the inductor current before and after changes in the R_{TEG}, respectively. Also, V_{in0} and V_{in1} are input voltage of the converter before and after changes.

Considering the TEG model in Figure 2, it is clear that

$$R_{TEG} = -\frac{V_{in1} - V_{in0}}{X_1 - X_0} \tag{27}$$

$$V_{oc} = R_{TEG} X_0 + V_{in0} = R_{TEG} X_1 + V_{in1} \tag{28}$$

By the measurement of the system operating point on $t = t_0$ as (X_0, V_{in0}) and $t = t_1$ as (X_1, V_{in1}), the values of the R_{TEG} and V_{oc} can be calculated from (27) and (28), respectively. After updating values of the mentioned parameter in the controller (in Equations (22) to (24)), MPP operation of the TEG system can be achieved.

4 | SIMULATION AND EXPERIMENTAL RESULTS

To investigate the response of the proposed backstepping controller in Figure 4, it is simulated in Matlab/Simulink software.

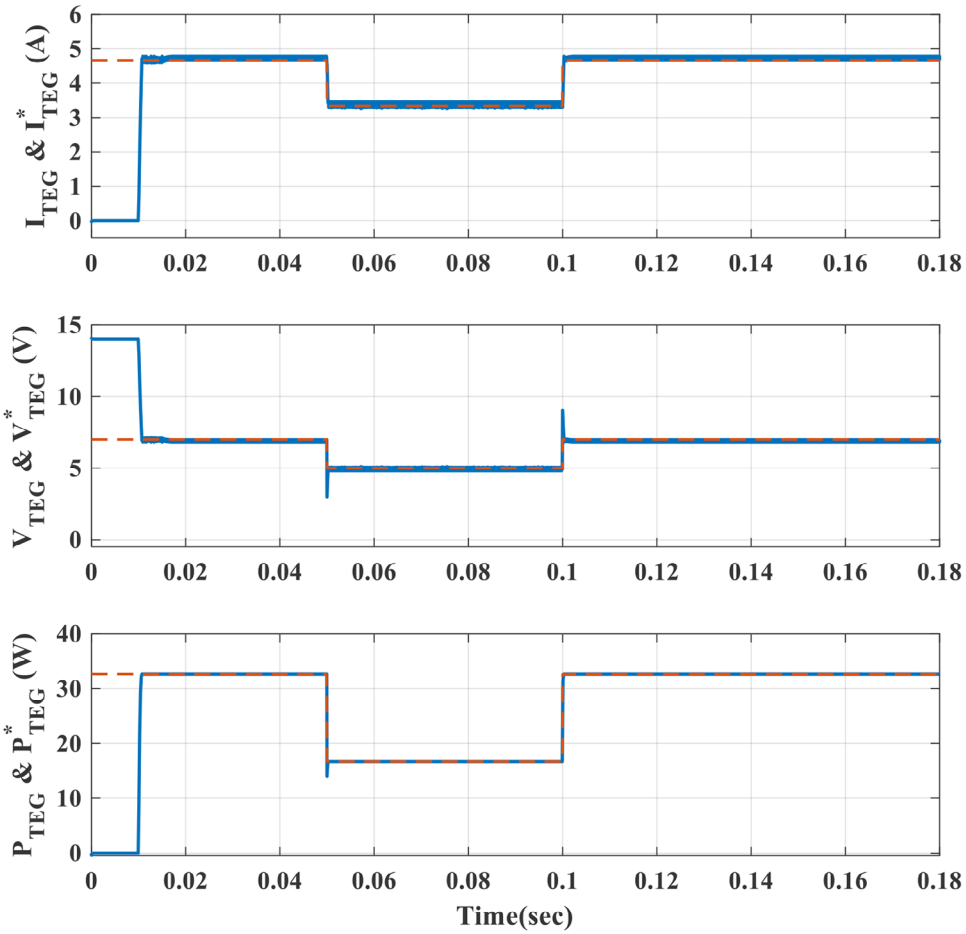

FIGURE 17 Response of the proposed non-linear resistance controller to step changes of TEG voltage (V_{OC} is stepped down from 14 to 10 V at $t = 0.05$ s, and then stepped up from 10 to 14 V at $t = 0.1$ s.). The MPPT controller is activated at $t = 0.01$ s. MPPT, maximum power point tracking; TEG, thermoelectric generator.

Also, the details of the implemented closed-loop system and the controller are illustrated in Figure 7. Considering the equivalent model of power source in Figure 1, a TEG simulator is employed as an input power source, which is described in Figure 8. By switching S1 and S2 ON/OFF, the step response of the closed-loop system can be evaluated against variation of the TEG resistance (R_{TEG}) and open-circuit voltage (V_{OC}).

Details of experimental setup including the block diagram of closed-loop system as well as the flowchart of designed controller are illustrated in Figure 7. Also, the power circuit of TEG simulator is shown in Figure 8. It is employed for controller evaluation against step changes of TEG open-circuit voltage and internal resistance. In Figure 8, IRFP460 (and its internal diode) is used for the implementation of the power switches. In the TEG simulator, switching the S_1 will lead to step changes of internal resistance (R_{TEG}) between 1.5 and 2.3 **Ω**. Moreover, S_2 is used for step changes of open-circuit voltage. To control the step-up converter and achieve MPPT of the input source, the TEG current is measured by LA55-P isolated Hall Effect sensors at first. Moreover, IRFP460 MOSFET and its internal diode, BP17-12 battery are used for the implementation of the power circuit and load respectively. The proposed controller is implemented by using the DSP (TMS320F28335) from Texas Instrument. An internal Pulse Width Modulation (PWM) unit of the DSP is used for switching signal generation. As an interface between the DSP unit and power switches, the HCPL-316 is used for the implementation of the gate driver circuit.

During the converter start-up, nominal system parameters are used for the calculation of the control effort (duty cycle). As values of the R_{TEG} and V_{OC} are changed by the variation of the temperature gradient, the controller updates these parameters each 100 ms. It should be noted that the converter switching frequency is 20 kHz.

It should be noted that experimental results are recorded by using a 20-MHz oscilloscope. Internal variables of the DSP including maximum input power as well as control effort are monitored through a digital-to-analogue converter (D/A) in the experimental setup. A photo of the test rig is presented in Figure 9.

Test 1—Start-up response with nominal parameters

In this test, the response of developed backstepping controller is illustrated from the converter start-up point. It is assumed that the switches S_1 and S_2 are ON in the TEG simulator (Figure 8) and hence, R_{TEG} = 1.5 Ω and V_{OC} = 14 V. Also in this test, real TEG parameters are used for the calculation of the designed controller. So, it is not necessary to update these parameters for MPPT of the TEG source. Considering nominal values of the system, input current and voltage of the input power source are $x_1 = \frac{V_{OC}}{2R_{TEG}} = \frac{14}{2\times1.5} = 4.67$ A and $V_{in} = \frac{V_{OC}}{2} = 7$ V in MPP of the system. Moreover, maximum power of the TEG is $P_m = x_1\ V_{in} = 32.67$ W. The simulation and experimental responses of the proposed closed-loop controller are illustrated in Figures 10 and 11. It is seen that before start-up, input current of the TEG source is zero and $V_{in} = V_{OC} = 14$. According to the simulation and experimental responses, although the value of the battery voltage is an uncertain parameter, it is seen that the designed backstepping controller is able to track MPP of the TEG source without steady-state error and reasonable dynamic response during the converter start-up. Finally, according to Figure 11d, the maximum value of the duty-cycle is limited to 0.95 during transient conditions Figures 12 and 13.

Test 2—Start-up response with unknown parameters of the TEG source

Similar to the previous test, it is assumed that the switches S_1 and S_2 are ON in the TEG simulator (Figure 8) and hence, R_{TEG} = 1.5 Ω and V_{OC} = 14 V. However, as the values of these parameters are uncertain, different values for the mentioned parameters are considered R_{TEG} = 2 Ω and V_{OC} = 5 V. Therefore, after start-up, the controller is not able to track the MPP of the TEG source properly.

To obtain MPP operation of the converter, the value of the R_{TEG} is increased by 10% after 10 ms. Considering the input current and voltage of the TEG source, the actual values of the R_{TEG} and V_{OC} are calculated by using Equations (27) and (28) and finally, the operating point of the converter is settled at the MPP (Figures 12, 13).

It should be noted that in steady-state operation, the calculated value of R_{TEG} is changed by 15% each 100 ms in the DSP codes to determine the variation of TEG parameters. The steady-state response of the controller is illustrated in Figure 14. Finally, it should be noted that the calculation interval is 5 ms.

Test 3—Controller response to step changes of the TEG resistance

It is assumed that the switch S_2 is ON in the TEG simulator (Figure 8) and the open-circuit voltage is 14 V. In this condition, despite changes of R_{TEG}, the input voltage of the converter should be settled on $V_{in} = \frac{V_{OC}}{2} = 7$ V for MPPT of the source. By switching S_1 in the TEG simulator, controller behaviour during step changes of the R_{TEG} can be investigated. According to the experimental response of the developed backstepping controller in Figure 14, despite wide changes of the R_{TEG}, it is seen that the closed-loop system can stabilize the input voltage of the chopper at MPP on 7 V. In the calculation interval in Figure 14, the values of the TEG parameters are updated in the controller.

Test 4—Open-circuit voltage changes

It is assumed that the switch S_1 is ON in the TEG simulator (Figure 7) and R_{TEG} is equal to 1.5 Ω. By switching the S_2 in the TEG simulator, the response of the proposed closed-loop system to V_{OC} step changes is studied. While the V_{OC} is equal to10 V, the MPP of converter will be $V_{in} = \frac{V_{OC}}{2} = 5V$ and $x_1 = \frac{V_{OC}}{2R_{TEG}} = 3.33A$. Similarly, for V_{OC} = 14, the MPP is V_{in} = 7 V and x_1 = 4.67 A. Furthermore, maximum power of the converter is P_m = 16.65 and 32.69 W, respectively.

According to the experimental result of the proposed controller in Figure 15, in spite of changes of Voc, it is seen that the controller is able to stabilize the input current and voltage of the converter at the MPP.

4.1 | Comparison and Discussion

According to our research on MPPT of TEG sources, the application of a non-linear closed-loop controller for input resistance control of the DC–DC boost converter is a novel idea and there is not any published report on input resistance control of the DC–DC converters. For this reason, the proposed method is compared with the P&O-based two-loop control approach [29] which is widely used for MPPT of PV and TEG systems in commercial/industrial applications. The detail of two-loop P&O-based MPPT is shown in Figure 16.

According to Figure 16, the P&O approach is employed for the calculation of TEG reference voltage (V_{mpp}) at MPP in the outer loop. Also, a PI controller is used in the inner loop of two-loop controller to satisfy the $V_{in} = V_{mpp}$. It is assumed that the voltage perturbations are 0.1 V and the proportional and integral gains of PI controller are 1 and 5, respectively.

Considering the following criteria, the proposed non-linear resistance controller is compared with the two-loop P&O approach:

A. The start-up response
B. The step changes of TEG open-circuit voltage (the V_{OC} value is stepped down from 14 to 7 V, and then stepped up from 7 to 14 V.)

Considering the mentioned criteria, the response of the proposed non-linear resistance controller is illustrated in Figure 17. At first, considering the nominal parameters of the power circuit, it is assumed that the controller is not enabled, and its

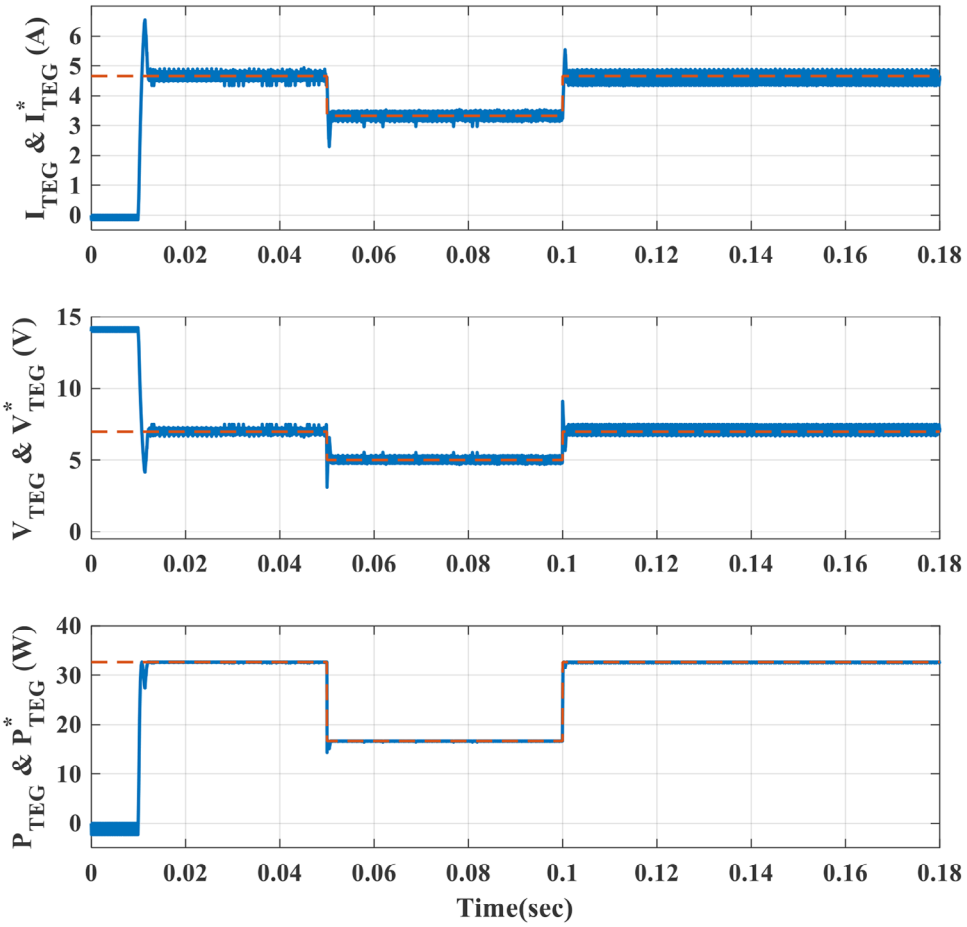

FIGURE 18 Response of the P&O-based two-loop MPPT controller to step changes of TEG voltage (V_{OC} is stepped down from 14 to 10 V at $t = 0.05$ s, and then stepped up from 10 to 14 V at $t = 0.1$ s.). The MPPT controller is activated at $t = 0.01$ s. MPPT, maximum power point tracking; P&O, perturb and observe; TEG, thermoelectric generator.

output is not applied to the power switch. Hence, as the controller is not active, the TEG current is zero and the voltage is 14 V (equal to V_{OC}). Then at $t = 0.01$ s, the controller is activated.

The desired value of the TEG voltage and current will be equal to

$$V_{mpp} = \frac{V_{OC}}{2} = 7\ \text{V}$$

$$I_{mpp} = \frac{V_{OC}}{2R_{TEG}} = \frac{14}{2 \times 1.5} = 4.67\ \text{A}$$

In this condition, TEG power is equal to 32.67 W.

At $t = 0.05$, V_{OC} is stepped down to 10 V, and at $t = 0.1$ s, it is stepped up to the nominal value ($V_{OC} = 14$ V). Despite 40% changes in the open-circuit voltage, it is seen that the proposed controller is stable and robust against parameter changes with zero steady-state error.

Also, the response of P&O-based two-loop controller under the same test condition is illustrated in Figure 18.

Comparing the simulation results in Figures 17 and 18, it can be concluded that

1. The dynamic response of the proposed controller is faster than the P&O-based two-loop controller.
2. The response fluctuation of the P&O approach within the steady-state condition can be removed using the developed non-linear controller.

5 | CONCLUSION

For MPPT of thermoelectric devices, a novel non-linear backstepping controller is presented for input resistance control of the step-up chopper. Considering the Lyapunov criteria, the asymptotic stability of developed non-linear controller is proved using the Barbalat lemma. To evaluate the response of designed backstepping controller against step changes of the open-circuit voltage and internal resistance, a simple TEG simulator is employed in the experimental tests. During the steady-state operation, the actual values of the V_{OC} and R_{TEG} are updated periodically by the measurement of the converter input voltage/current. To verify the functionality of the developed control method, some PC-based simulations are carried out in MATLAB/Simulink software. Moreover, by using TMS320F2810

DSP from Texas Instruments, the experimental response of the proposed controller is evaluated in the dynamic and steady-state conditions. A developed closed-loop system can track the MPP of TEG with zero steady-state error, regardless of uncertain parameter variations.

AUTHOR CONTRIBUTIONS

Sarah Kowsari Moghadam: Formal analysis; data curation; writing—original draft; visualization. **Mahdi Salimi**: Conceptualization; methodology; software; Validation; investigation; supervision; project administration; writing-review & editing. **Seyyed Mohammad Taghi Bathaee**: Supervision; writing—review & editing. **Davar Mirabasi**: Supervision; writing—review & editing.

CONFLICT OF INTEREST STATEMENT

The authors declare no conflict of interest.

ACKNOWLEDGEMENTS

This research received no specific grant from any funding agency in the public, commercial, or not-for-profit sectors.

DATA AVAILABILITY STATEMENT

All data presented in this manuscript has been generated by authors through MATLAB simulation or experimental implementation.

ORCID

Mahdi Salimi https://orcid.org/0000-0003-3007-3027

REFERENCES

1. Ortiz-Imedio, R., Caglayan, D.G., Ortiz, A., Heinrichs, H., Robinius, M., Stolten, D., Ortiz, I.: Power-to-Ships: Future electricity and hydrogen demands for shipping on the Atlantic coast of Europe in 2050. Energy 228, 120660 (2021). ISSN 0360–5442. https://doi.org/10.1016/j.energy.2021.120660
2. Shen, Z.-G., Wu, S.-Y., Xiao, L., Chen, Z.-X.: Proposal and assessment of a solar thermoelectric generation system characterized by Fresnel lens, cavity receiver and heat pipe. Energy 141, 215–238 (2017). ISSN 0360–5442. https://doi.org/10.1016/j.energy.2017.09.051
3. Lefranc, G., et al.: Waste heat recovery plant for exhaust ducts using thermoelectric generators. IEEE Lat. Am. Trans. 14(6), 2752–2757 (2016). https://doi.org/10.1109/TLA.2016.7555249
4. Twaha, S., Zhu, J., Yan, Y., Li, B.: A comprehensive review of thermoelectric technology: Materials, applications, modelling and performance improvement. Renew. Sustain. Energy Rev. 65, 698–726 (2016)
5. Sasaki, K., Horikawa, D., Goto, K.: Consideration of thermoelectric power generation by using hot spring thermal energy or industrial waste heat. J. Electron. Mater. 44, 391–398 (2015). https://doi.org/10.1007/s11664-014-3189-z
6. Singh, G.K.: Solar power generation by PV (photovoltaic) technology: A review. Energy 53, 1–13 (2013). ISSN 0360–5442. https://doi.org/10.1016/j.energy.2013.02.057
7. Selvakumar, S., Madhusmita, M., Koodalsamy, C., Simon, S.P., Sood, Y.R.: High-speed maximum power point tracking module for PV systems. IEEE Trans. Ind. Electron. 66(2), 1119–1129 (2019). https://doi.org/10.1109/TIE.2018.2833036
8. Salimi, M.: Practical implementation of the Lyapunov based nonlinear controller in step-up DC-DC chopper for MPPT of the PV systems. Sol. Energy 173, 246–255 (2018). ISSN 0038–092X. https://doi.org/10.1016/j.solener.2018.07.078
9. Taheri, H., Taheri, S.: Two-diode model-based nonlinear MPPT controller for PV systems. Can. J. Electr. Comput. Eng. 40(2), 74–82 (2017). https://doi.org/10.1109/CJECE.2016.2606357
10. Meng, Z., Shao, W., Tang, J., Zhou, H.: Sliding-mode control based on index control law for MPPT in photovoltaic systems. CES Trans. Electr. Mach. Syst. 2(3), 303–311 (2018). https://doi.org/10.30941/CESTEMS.2018.00038
11. Hussain, A., Garg, M.M., Korukonda, M.P., Hasan, S., Behera, L.: A parameter estimation based MPPT method for a PV system using Lyapunov control scheme. IEEE Trans. Sustain. Energy 10(4), 2123–2132 (2019). https://doi.org/10.1109/TSTE.2018.2878924
12. Montoya, D.G., Ramos-Paja, C.A., Giral, R.: Improved design of sliding-mode controllers based on the requirements of MPPT techniques. IEEE Trans. Power Electron. 31(1), 235–247 (2016). https://doi.org/10.1109/TPEL.2015.2397831
13. Ramasamy, A., Suthanthira Vanitha, N.: Maximum power tracking for PV generating system using novel optimized fractional order open circuit voltage- FOINC method. In: 2014 International Conference on Computer Communication and Informatics, Coimbatore, pp. 1–6 (2014). https://doi.org/10.1109/ICCCI.2014.6921842
14. Kolesnik, S., Kuperman, A.: On the equivalence of major variable-step-size MPPT algorithms. IEEE J. Photovoltaics 6(2), 590–594 (2016). https://doi.org/10.1109/JPHOTOV.2016.2520212
15. Kim, J., Kim, C.: A DC–DC boost converter with variation-tolerant MPPT technique and efficient ZCS circuit for thermoelectric energy harvesting applications. IEEE Trans. Power Electron. 28(8), 3827–3833 (2013)
16. Montecucco, A., Knox, A.R.: Maximum power point tracking converter based on the open-circuit voltage method for thermoelectric generators. IEEE Trans. Power Electron. 30(2), 828–839 (2015). https://doi.org/10.1109/TPEL.2014.2313294
17. Rodriguez, R., Guo, J., Preindl, M., Cotton, J.S., Emadi, A.: High frequency injection maximum power point tracking for thermoelectric generators. Energy Convers. Manage. 198, 111832 (2019). ISSN 0196–8904. https://doi.org/10.1016/j.enconman.2019.111832
18. Bijukumar, B., Raam, A.G.K., Ganesan, S.I., Nagamani, C.: A linear extrapolation-based MPPT algorithm for thermoelectric generators under dynamically varying temperature conditions. IEEE Trans. Energy Convers. 33(4), 1641–1649 (2018). https://doi.org/10.1109/TEC.2018.2830796
19. Qian, Y., Zhang, H., Chen, Y., Qin, Y., Lu, D., Hong, Z.: A SIDIDO DC–DC converter with dual-mode and programmable-capacitor-array MPPT control for thermoelectric energy harvesting. IEEE Trans. Circuits Syst. II Express Briefs 64(8), 952–956 (2017). https://doi.org/10.1109/TCSII.2016.2627551
20. Carreon-Bautista, S., Eladawy, A., Nader Mohieldin, A., Sánchez-Sinencio, E.: Boost converter with dynamic input impedance matching for energy harvesting with multi-array thermoelectric generators. IEEE Trans. Ind. Electron. 61(10), 5345–5353 (2014). https://doi.org/10.1109/TIE.2014.2300035
21. Li, F., Lin, D., Yu, T., Li, J., Wang, K., Zhang, X., Yang, B., Wu, Y.: Adaptive rapid neural optimization: A data-driven approach to MPPT for centralized TEG systems. Electr. Power Syst. Res. 199, 107426 (2021). ISSN 0378–7796. https://doi.org/10.1016/j.epsr.2021.107426
22. Xu, W., Wang, A., Lin, S., Li, J., Wei, B., Duan, J., Sun, X., Liu, J.: An internal-resistance-adaptive MPPT circuit for energy harvesting. AEU – Int. J. Electron. Commun. 127, 153464 (2020). ISSN 1434–8411. https://doi.org/10.1016/j.aeue.2020.153464
23. Mei, Q., Shan, M., Liu, L., Guerrero, J.M.: A novel improved variable step-size incremental-resistance MPPT method for PV systems. IEEE Trans. Ind. Electron. 58(6), 2427–2434 (2011). https://doi.org/10.1109/TIE.2010.2064275
24. Rezk, H., Harrag, A.: A robust type-2 fuzzy logic-based maximum power point tracking approach for thermoelectric generation systems. Int. J. Energy Res. 45(12), 18066–18080 (2021). https://doi.org/10.1002/er.6955
25. Kwan, T.H., Wu, X., Yao, Q.: Integrated TEG-TEC and variable coolant flow rate controller for temperature control and energy harvesting. Energy 159, 448–456 (2018). ISSN 0360–5442. https://doi.org/10.1016/j.energy.2018.06.206

26. Rahman, Z.H.A., Khir, M.H.M., Burhanudin, Z.A.: Modeling and simulation analysis of micro thermoelectric generator. In: 2016 6th International Conference on Intelligent and Advanced Systems (ICIAS), Kuala Lumpur, pp. 1–5 (2016). https://doi.org/10.1109/ICIAS.2016.7824110
27. Bond, M., Park, J.: Current-sensorless power estimation and MPPT implementation for thermoelectric generators. IEEE Trans. Ind. Electron. 62(9), 5539–5548 (2015). https://doi.org/10.1109/TIE.2015.2414393
28. Salimi, M., Soltani, J., Markadeh, G.A., Abjadi, N.R.: Indirect output voltage regulation of DC-DC buck/boost converter operating in continuous and discontinuous conduction modes using adaptive backstepping approach. IET Power Electron. 6(4), 732–741 (2013). https://doi.org/10.1049/iet-pel.2012.0198
29. Hanzaei, S.H., Gorji, S.A., Ektesabi, M.: A scheme-based review of MPPT techniques with respect to input variables including solar irradiance and PV arrays' temperature. IEEE Access 8, 182229–182239 (2020). https://doi.org/10.1109/ACCESS.2020.3028580

How to cite this article: Mogadam, S.K., Salimi, M., Bathaee, S.M.T., Mirabasi, D.: Experimental evaluation of the backstepping-based input resistance controller in step-up DC–DC converter for maximum power point tracking of the thermoelectric generators. IET Power Electron. 1–17 (2023).
https://doi.org/10.1049/pel2.12628